simple GA is slow to evolve but after 120 generations (18,000 function evaluations) reaches a near-optimal solution. The boundary conditions for the best solution in the simple GA are $r(t_f) = 1.519$ DU, $\theta(t_f) = 147.18$ deg, $u(t_f) = 0.005$ DU/TU, and $v(t_f) = 0.807$ DU/TU and for the μGA with a population of 15 are $r(t_f) = 1.514$ DU, $\theta(t_f) = 162.59$ deg, $u(t_f) = 0.206$ DU/TU, and $v(t_f) = 0.805$ DU/TU. The μGAs' radial position and tangential velocity are close to the desired values given in Eq. (14) but the radial velocity would make the final orbit eccentric.

Results: Inequality Constraints Method

Figure 1 also displays the objective function for the best individual in the population using inequality constraints. The vertical scale on the right should be used. It is seen that, given a sufficient number of generations, all three GAs converged to a near-optimal solution. However, the μGAs converged to the near-optimal region more quickly than did the simple GA. The performance of all GAs became comparable after approximately 7500 function evaluations. The boundary conditions for best solution in the μGA with a population of 15 after 6000 are $r(t_f) = 1.509$ DU, $\theta(t_f) = 153.41$ deg, $u(t_f) = 0.042$ DU/TU, and $v(t_f) = 0.808$ DU/TU and after 12,000 function evaluations are $r(t_f) = 1.524$ DU, $\theta(t_f) = 152.59$ deg, $u(t_f) = 0.051$ DU/TU, and $v(t_f) = 0.807$ DU/TU.

Orbital rendezvous trajectories have also been solved using μGAs with inequality constraints but are not shown here. In all cases the μGA provides an extremely fast approach to a near-optimal trajectory.

Conclusions

The use of μGAs to determine near-optimal low-thrust trajectories was explored. Micro-GAs were inefficient at achieving near-optimal solutions when boundary conditions were treated as equality constraints. However, when boundary conditions were cast as inequality constraints, μGAs showed faster convergence than did simple GAs to a near-optimal region.

Acknowledgment

The author would like to acknowledge David Carroll for providing the GA driver used in this study and for valuable discussions pertaining to its use.

References

[1]Gage, P. J., Braun, R. D., and Kroo, I. M., "Interplanetary Trajectory Optimization Using a Genetic Algorithm," *Journal of the Astronautical Sciences*, Vol. 43, No. 1, 1995, pp. 59–75.

[2]Carter, M. T., and Vadali, S. R., "Parameter Optimization Using Adaptive Bound Genetic Algorithms," American Astronomical Society, Spaceflight Mechanics Conf., AAS Paper 95-140, Albuquerque, NM, Feb. 1995.

[3]Pinon, E., III, and Fowler, W. T., "Lunar Launch Trajectory Optimization Using a Genetic Algorithm," American Astronomical Society, Spaceflight Mechanics Conf., AAS Paper 95-142, Albuquerque, NM, Feb. 1995.

[4]Rauwolf, G., and Coverstone-Carroll, V., "Near-Optimal Low-Thrust Orbit Transfers Generated by a Genetic Algorithm," *Proceedings of the 18th Southeastern Conference on Theoretical and Applied Mechanics*, Univ. of Alabama, Tuscaloosa, AL, 1996, pp. 431–442.

[5]Goldberg, D. E., *Genetic Algorithms in Search, Optimization and Machine Learning*, Addison–Wesley, Reading, MA, 1989, pp. 112, 113.

[6]Goldberg, D. E., "Sizing Populations for Serial and Parallel Genetic Algorithms," *Proceedings of Third International Conference on Genetic Algorithms* (Fairfax, VA), Clearinghouse for Genetic Algorithms, Dept. of Engineering Mechanics, Univ. of Alabama, Tuscaloosa, AL, 1989, pp. 70–79.

[7]Krishnakumar, K., "Micro-Genetic Algorithms for Stationary and Non-Stationary Function Optimization," Society of Photo-Optical Instrumentation Engineers, Conf. on Intelligent Control and Adaptive Systems, SPIE Paper 1196-32, Philadelphia, PA, Nov. 1989.

[8]Carroll, D. L., "Genetic Algorithms and Optimizing Chemical Oxygen-Iodine Lasers," *Proceedings of the 18th Southeastern Conference on Theoretical and Applied Mechanics*, Univ. of Alabama, Tuscaloosa, AL, 1996, pp. 411–430.

[9]Seywald, H., and Kumar, R.,"Genetic Algorithms and Equality Constrained Optimization Problems," *Journal of Guidance, Control, and Dynamics* (submitted for publication).

[10]Bryson, A. E., and Ho, Y. C., *Applied Optimal Control*, Hemisphere, New York, 1975, pp. 66–69.

[11]Holland, J., *Adaptation in Natural and Artificial Systems*, MIT Press, Cambridge, MA, 1992, Chap. 1.

[12]Bate, R. R., Mueller, D. D., and White, J. E., *Fundamentals of Astrodynamics*, Dover, New York, 1971, pp. 40, 41.

Conjecture About Orthogonal Functions

Larry Silverberg*
North Carolina State University, Raleigh, North Carolina 27695-7910

Introduction

I FIRST came upon this result in my work in the area of control of distributed systems. I was studying the manner in which the natural modes of vibration of simple beams are altered by attaching to them concentrated spring and damping elements. The result has since been distilled into an unproven theorem, presently being called the orthogonal function conjecture.

Orthogonal function conjecture: Let $\phi_r(x)$ $(r = 1, 2, \ldots, n+1)$ be an ordered set of real orthonormal functions defined over the interval $[a, b]$. The zeros of the $(n+1)$th orthonormal functions are $x_r (r = 1, 2, \ldots, n)$. Then an orthonormal set of n real n-dimensional orthonormal vectors can be constructed from the orthonormal functions by evaluating the lowest n orthonormal functions at the zeros of the $(n+1)$th orthonormal function. The orthonormal vectors are $\psi_r = [w_1\phi_r(x_1)\ \ w_2\phi_r(x_2)\ \ \cdots\ \ w_n\phi_r(x_n)]^T$ $(r = 1, 2, \ldots, n)$ in which w_r $(r = 1, 2, \ldots, n)$ are positive numbers.

This described orthogonal function conjecture is both unusual and a paradox. It is unusual because the zeros of the $(n+1)$th orthonormal function influence the construction of orthonormal vectors from the lowest n orthonormal functions. The orthogonal function conjecture is a paradox for reasons described in the next section.

Paradox

Let us now more closely examine the orthogonal function conjecture. The orthonormality conditions that the functions $\phi_r(x)$ satisfy are given by

$$\int_0^1 \phi_r(x)\phi_s(x)\,dx = \delta_{rs} \qquad (r, s = 1, 2, \ldots, n+1) \tag{1}$$

where δ_{rs} is the Kronecker delta function ($\delta_{rs} = 0$ when $r \neq s$ and $\delta_{rr} = 1$) and x is defined over the interval $[0, 1]$. The zeros of $\phi_{n+1}(x)$ satisfy

$$\phi_{n+1}(x_t) = 0 \qquad (t = 1, 2, \ldots, n) \tag{2}$$

It is implied by Eq. (2) that $\phi_{n+1}(x)$ has n zeros. The n-dimensional orthonormal vectors are stated in the conjecture to satisfy the orthonormality conditions

$$\psi_r^T\psi_s = \delta_{rs} \qquad (r, s = 1, 2, \ldots, n) \tag{3}$$

where $\psi_r = [w_1\phi_r(x_1)\ \ w_2\phi_r(x_2)\ \ \cdots\ \ w_n\phi_r(x_n)]^T$ in which w_r shall be referred to as weighting constants. The paradox arises when we recognize that Eq. (3) represents a set of linear algebraic equations in terms of the unknowns w_r^2 $(r = 1, 2, \ldots, n)$. The number of equations is equal to n^2, and the equation corresponding to the pair of indices (r, s) is identical to the equation corresponding to the pair of indices (s, r). Therefore, the number of independent equations is $N = n(n+1)/2$. The paradox lies in that the number of equations

Received July 30, 1995; revision received May 10, 1996; accepted for publication Sept. 16, 1996.

*Professor, Department of Mechanical and Aerospace Engineering. Member AIAA.

is larger than the number of unknowns (when $n > 1$). Indeed, the existence of an exact solution to an overdetermined set of linear algebraic equations is altogether unexpected. Without an available explanation, the presence of an exact solution must be regarded as a paradox.

Sine Functions

Without a proof of the orthogonal function conjecture, I now resort to verifying the conjecture. The verification is given to provoke insight that could lead to a proof of the conjecture at a later date. The verification could also illuminate restrictive conditions to which the conjecture is subject. First consider the orthonormal set of sine functions

$$\phi_r(x) = \sqrt{2}\sin r\pi x \qquad (r = 1, 2, \ldots, n+1) \tag{4}$$

The zeros of $\phi_{n+1}(x)$ are

$$x_t = t/(n+1) \qquad (t = 1, 2, \ldots, n) \tag{5}$$

The weights w_r $(r = 1, 2, \ldots, n)$ associated with the orthonormal vectors ψ_r $(r = 1, 2, \ldots, n)$ are obtained by letting $r = s$ in Eq. (3). This yields the set of n linear algebraic equations

$$\sum_{t=1}^{n} \phi_r^2(x_t) w_t^2 = 1 \qquad (r = 1, 2, \ldots, n) \tag{6}$$

Letting $r \neq s$ in Eq. (3) yields the unproven identities

$$\sum_{t=1}^{n} \phi_r(x_t)\phi_s(x_t) w_t^2 = 0 \qquad (r \neq s = 1, 2, \ldots, n) \tag{7}$$

Substituting Eqs. (4) and (5) into Eqs. (6) and (7), we get

$$\sum_{t=1}^{n} 2\sin^2\left(\frac{r\pi t}{n+1}\right) w_t^2 = 1 \qquad (r = 1, 2, \ldots, n) \tag{8}$$

and

$$\sum_{t=1}^{n} \sin\left(\frac{r\pi t}{n+1}\right)\sin\left(\frac{s\pi t}{n+1}\right) w_t^2 = 0 \qquad (r \neq s = 1, 2, \ldots, n) \tag{9}$$

As an illustration, let $n = 3$, in which case Eqs. (8) and (9) reduce to

$$\begin{bmatrix} 1 & 2 & 1 \\ 2 & 0 & 2 \\ 1 & 2 & 1 \end{bmatrix} \begin{Bmatrix} w_1^2 \\ w_2^2 \\ w_3^2 \end{Bmatrix} = \begin{Bmatrix} 1 \\ 1 \\ 1 \end{Bmatrix} \tag{10a}$$

$$\begin{bmatrix} \sqrt{2} & 0 & -\sqrt{2} \\ 1 & -2 & 1 \\ \sqrt{2} & 0 & -\sqrt{2} \end{bmatrix} \begin{Bmatrix} w_1^2 \\ w_2^2 \\ w_3^2 \end{Bmatrix} = \begin{Bmatrix} 0 \\ 0 \\ 0 \end{Bmatrix} \tag{10b}$$

Observe that the first and third equations in Eq. (10a) are identical to each other. The general solution to Eq. (10a) is then expressed in terms of w_1^2 as $(w_1^2 \;\; w_2^2 \;\; w_3^2) = (w_1^2 \tfrac{1}{4} \tfrac{1}{2} - w_1^2)$. Substituting the general solution to Eq. (10a) into Eq. (10b) verifies Eq. (10b) when $w_1 = \frac{1}{2}$. The verification of Eq. (9) for values of n ranging from 1 to 10 was carried out elsewhere.[1,2]

At this point in the verification, one might speculate that the satisfaction of Eq. (9) is peculiar to the sine functions given in Eq. (4). Let us look at another orthonormal set of sine functions, given by

$$\phi_r(x) = \sqrt{\frac{2\left(\beta_r^2 + \gamma^2\right)}{\beta_r^2 + \gamma^2 + \gamma}}\sin\beta_r x \tag{11a}$$

$$\beta_r \cot\beta_r + \gamma = 0 \qquad (r = 1, 2, \ldots, n+1) \tag{11b}$$

in which $\gamma > 0$ (Ref. 3). The zeros of $\phi_{n+1}(x)$ satisfy

$$x_t = \frac{\pi}{2\beta_{n+1}}(2t-1) \qquad (t = 1, 2, \ldots, n) \tag{12}$$

in which β_{n+1} is obtained from Eq. (11b). Substituting Eqs. (11a) and (12) into Eqs. (6) and (7) yields

$$\sum_{t=1}^{n} \frac{2\left(\beta_r^2 + \gamma^2\right)}{\beta_r^2 + \gamma^2 + \gamma}\sin^2\left[\frac{\beta_r}{\beta_{n+1}}\frac{\pi}{2}(2t-1)\right] w_t^2 = 1 \qquad (r = 1, 2, \ldots, n) \tag{13}$$

and

$$\sum_{t=1}^{n} \sqrt{\frac{4\left(\beta_r^2 + \gamma^2\right)\left(\beta_s^2 + \gamma^2\right)}{\left(\beta_r^2 + \gamma^2 + \gamma\right)\left(\beta_s^2 + \gamma^2 + \gamma\right)}}\sin\left[\frac{\beta_r}{\beta_{n+1}}\frac{\pi}{2}(2t-1)\right] \times \sin\left[\frac{\beta_s}{\beta_{n+1}}\frac{\pi}{2}(2t-1)\right] w_t^2 = 0 \qquad (r \neq s = 1, 2, \ldots, n) \tag{14}$$

As an illustration, let $n = 5$ and $\gamma = 2$. From Eq. (11b), $\beta_1 = 2.2889$, $\beta_2 = 5.0870$, $\beta_3 = 8.0962$, $\beta_4 = 11.1727$, $\beta_5 = 14.2764$, and $\beta_6 = 17.3932$. From Eq. (12), the zeros of ϕ_6 are given by $x_1 = 0.1806$, $x_2 = 0.3612$, $x_3 = 0.5419$, $x_4 = 0.7225$, and $x_5 = 0.9031$. By inversion of Eq. (13), the weighting constants $w_1 = 0.5158$, $w_2 = 0.4950$, $w_3 = 0.4700$, $w_4 = 0.4433$, and $w_5 = 0.4144$ are found. Substituting these values into the left-hand side of the unproven identities (14) completes the verification of the orthogonal function conjecture for the sine functions given by Eq. (11a) restricted to $n = 5$. The verification of Eq. (14) for values of n ranging from 1 to 15 was carried out elsewhere.[3]

The verification just given considered two orthonormal sets of sine functions. The sets of orthonormal functions for which the orthogonal function conjecture has been verified are given in Table 1. The orthogonal function conjecture was violated when the set of orthonormal functions was associated with free-free beams.[1] This set is a mixed set of two polynomial functions, and the remaining are transcendental functions. Observe in Table 1 that the orthogonal function conjecture was satisfied for another mixed set (case 4).

Isolated Proof for the Functions $\sqrt{2}\sin(r\pi x)$ $(r = 1, 2, \ldots, n+1)$

Although the author has presently failed to prove the orthogonal function conjecture with any level of generality, the set of functions $\sqrt{2}\sin(r\pi x)$ $(r = 1, 2, \ldots, n+1)$ is an isolated exception.

Toward this end, an attractive method of computing the weighting constants w_r $(r = 1, 2, \ldots, n)$ is first developed. The method avoids the matrix inverse that is required in Eq. (6). Adopting a matrix notation, and letting $\phi_{rs} = \phi_s(x_r)$ $(r, s = 1, 2, \ldots, n)$ denote the entries of $\boldsymbol{\Phi}$ and $w_{rs} = w_r\delta_{rs}$ $(r, s = 1, 2, \ldots, n)$ denote the entries of $\boldsymbol{W}$, the matrix counterpart to Eq. (3) becomes

$$\boldsymbol{\psi}^T\boldsymbol{\psi} = \boldsymbol{I} \tag{15a}$$

in which

$$\boldsymbol{\psi} = \boldsymbol{W}\boldsymbol{\Phi} \tag{15b}$$

where $\boldsymbol{I}$ is the $n \times n$ identity matrix. Substituting Eq. (15b) into Eq. (15a) yields $\boldsymbol{\Phi}^T\boldsymbol{W}^2\boldsymbol{\Phi} = \boldsymbol{I}$ since $\boldsymbol{W}^T\boldsymbol{W} = \boldsymbol{W}^2$. Premultiplying this result by $\boldsymbol{\Phi}^{-T}$, and postmultiplying this result by $\boldsymbol{\Phi}^{-1}$ (assuming that $\boldsymbol{\Phi}^{-1}$ exists), leads to $\boldsymbol{W}^2 = \boldsymbol{\Phi}^{-T}\boldsymbol{\Phi}^{-1} = (\boldsymbol{\Phi}\boldsymbol{\Phi}^T)^{-1}$, which upon inversion yields

$$\boldsymbol{W}^{-2} = \boldsymbol{\Phi}\boldsymbol{\Phi}^T \tag{16}$$

in which the entries of $\boldsymbol{W}^{-2}$ are $(1/w_r^2)\delta_{rs}$. Returning to an index notation, Eq. (16) becomes

$$\left(\frac{1}{w_r^2}\right)\delta_{rs} = \sum_{t=1}^{n} \phi_t(x_r)\phi_t(x_s) \qquad (r, s = 1, 2, \ldots, n) \tag{17}$$

When $r = s$, Eq. (17) is an attractive equation to use to determine w_r $(r = 1, 2, \ldots, n)$. When $r \neq s$, Eq. (17) represents an alternate form of the unproven identities (7). Thus, from now on a proof of Eq. (17)

Table 1 Verification of orthogonal function conjecture

	Transcendental functions	
1)	$\phi_r(x) = \sqrt{2}\sin r\pi x, \quad 0 < x < 1 \quad (r = 1, 2, \ldots, n+1; n = 1, 2, \ldots, 10)$	(Refs. 1, 2)
2)	$\phi_r(x) = \sqrt{2}\sin\left[\dfrac{(2r-1)\pi x}{2}\right], \quad 0 < x < 1 \quad (r = 1, 2, \ldots, n+1; n = 1, 2, \ldots, 10)$	
3)	$\phi_r(x) = \sqrt{\dfrac{2\left(\beta_r^2+\gamma^2\right)}{\beta_r^2+\gamma^2+\gamma}}\sin\beta_r x, \quad \beta_r\cot\beta_r + \gamma = 0, \quad \gamma = 2, \quad 0 < x < 1$ $(r = 1, 2, \ldots, n+1; n = 1, 2, \ldots, 10)$	(Ref. 3)
4)	$\phi_0(x) = 1, \quad \phi_r(x) = \sqrt{2}\cos(r\pi x), \quad 0 < x < 1 \quad (r = 1, 2, \ldots, n+1; n = 1, 2, \ldots, 10)$	
5)	$\phi_r(x) = \sqrt{\dfrac{2\left(\beta_r^2+\gamma^2\right)}{\beta_r^2+\gamma^2+\gamma}}\cos\beta_r x, \quad 0 < x < 1, \quad \beta_r\tan\beta_r = \gamma, \quad \gamma = \dfrac{1}{5}$ $(r = 1, 2, \ldots, n+1; n = 1, 2, \ldots, 10)$	(Ref. 3)
6)	$\phi_r(x) = \left(\dfrac{\cos\beta_r + \cosh\beta_r}{\sin\beta_r + \sinh\beta_r}\right)(\sin\beta_r x - \sinh\beta_r x) + \cosh\beta_r x - \cos\beta_r x$ $1 + \cos\beta_r\cosh\beta_r = 0, \quad 0 < x < 1 \quad (r = 1, 2, \ldots, n+1; n = 1, 2, \ldots, 10)$	(Ref. 1)
	Polynomial functions	
7)	$\phi_1(x) = 1, \quad \phi_2(x) = 2\sqrt{3}x, \quad \phi_3(x) = 6\sqrt{5}\left(x^2 - \frac{1}{12}\right), \quad \phi_4(x) = 20\sqrt{7}\,x\left(x_2 - \frac{3}{20}\right)$ $\phi_5(x) = 210(x^4 - 3x^2/14 + 3/560), \ldots, -\frac{1}{2} < x < \frac{1}{2}$ (Legendre polynomials) $\quad (n = 1, 2, \ldots, 10)$	(Ref. 1)

is sought when $r \neq s$, restricting our attention to the orthonormal set of functions $\sqrt{2}\sin(r\pi x)$ $(r = 1, 2, \ldots, n+1)$.

Within our restrictive context, Eq. (17) for $r \neq s$ reduces to

$$0 = \sum_{t=1}^{n} 2\sin\frac{rt\pi}{n+1}\sin\frac{st\pi}{n+1} = \sum_{t=1}^{n}\left[\cos\frac{(r-s)\pi t}{n+1} - \cos\frac{(r+s)\pi t}{n+1}\right] \qquad (r \neq s = 1, 2, \ldots, n) \tag{18}$$

When $r \pm s = 2k$ is even, the identity

$$\sum_{t=0}^{n}\cos\frac{2\pi kt}{n+1} = 0 \qquad (k = 1, 2, \ldots, n)$$

can be used to show that

$$\sum_{t=1}^{n}\cos\frac{(r \pm s)\pi t}{n+1} = -1$$

It follows that Eq. (18) is satisfied when $r \pm s$ is even. It remains to prove Eq. (18) when $r \pm s = k$ is odd. First, consider the even n cases, for which

$$\sum_{t=0}^{n+1}\cos\frac{\pi kt}{n+1} = \sum_{t=0}^{n/2}\cos\frac{\pi kt}{n+1} + \sum_{t=(n+2)/2}^{n+1}\cos\frac{\pi kt}{n+1}$$

$$= \sum_{t=0}^{n/2}\cos\frac{\pi kt}{n+1} - \sum_{t'=n/2}^{t'=0}\cos\frac{\pi kt'}{n+1}$$

letting $t' = n + 1 - t$. Then

$$\sum_{t=0}^{n+1}\cos\frac{\pi kt}{n+1} = \sum_{t=0}^{n/2}\cos\frac{\pi kt}{n+1} - \sum_{t=0}^{n/2}\cos\frac{\pi kt}{n+1} = 0$$

and so

$$\sum_{t=1}^{n}\cos\frac{\pi kt}{n+1} = \sum_{t=0}^{n+1}\cos\frac{\pi kt}{n+1} - \cos(0) - \cos(\pi k) = 0$$

for odd k. Finally, let us prove Eq. (18) for odd $r \pm s = k$ when n is odd. Under these conditions

$$\sum_{t=0}^{n+1}\cos\frac{\pi kt}{n+1} = \sum_{t=0}^{(n-1)/2}\cos\frac{\pi kt}{n+1} + \cos\frac{\pi k(n+1)/2}{n+1} - \sum_{t=(n+3)/2}^{n+1}\cos\left(-\frac{\pi kt}{n+1} + \pi k\right)$$

$$= \sum_{t=0}^{(n-1)/2}\cos\frac{\pi kt}{n+1} - \sum_{t'=(n-1)/2}^{t'=0}\cos\frac{\pi kt'}{n+1}$$

letting $t' = n + 1 - t$. Then

$$\sum_{t=0}^{n+1}\cos\frac{\pi kt}{n+1} = \sum_{t=0}^{(n-1)/2}\cos\frac{\pi kt}{n+1} - \sum_{t=0}^{(n-1)/2}\cos\frac{\pi kt}{n+1} = 0$$

so that for odd k

$$\sum_{t=1}^{n}\cos\frac{\pi kt}{n+1} = \sum_{t=0}^{n+1}\cos\frac{\pi kt}{n+1} - \cos(0) - \cos(\pi k) = 0$$

End of proof.

Node Control Conjecture

This section is for readers interested in the application of the orthogonal function conjecture; readers uninterested in this topic may wish to skip this section. An application of the orthogonal function conjecture to the control of distributed systems is now restated in the form of the node control conjecture. The node control conjecture was first presented in Ref. 1 and is presented again here to show how the orthogonal function conjecture can be used to determine control gains and to determine control input locations in direct state feedback control of one-dimensional systems. (The node control conjecture has been used to control transient temperatures in conducting media in Ref. 3 and to control vibration in two-dimensional plates and membranes in unpublished work by the authors of Ref. 2.)

Consider the partial differential equation that governs the transient vibration of a one-dimensional uniform bar

$$m\frac{\partial^2 u(x,t)}{\partial t^2} - AE\frac{\partial^2 u(x,t)}{\partial x^2} = f(x,t) \tag{19}$$

where $u(x,t)$ is a longitudinal displacement at $0 < x < 1$ and time $t > 0$, $f(x,t)$ is the control force distribution, m is the mass distribution, and AE is the stiffness distribution. Both m and AE are positive constants. The uniform bar is subject to the boundary conditions

$$-k_1 u(0,t) + \frac{\partial u(0,t)}{\partial x} = 0, \qquad k_2 u(1,t) + \frac{\partial u(1,t)}{\partial x} = 0 \tag{20}$$

in which k_1 and k_2 are nonnegative constants. The control force distribution is

$$f(x,t) = -\sum_{i=1}^{n}\left[g_i u(x,t) + h_i\frac{\partial u(x,t)}{\partial t}\right]\delta(x - x_i) \tag{21}$$

in which $\delta(x - x_i)$ is a spatial impulse at the undetermined location x_i and g_i and h_i are undetermined control gains. The eigenfunctions of the uniform bar solve the eigenvalue problem

$$\lambda^2 m\phi(x) - AE\frac{\mathrm{d}^2\phi(x)}{\mathrm{d}x^2} = -\sum_{i=1}^{n}(g_i + \lambda h_i)\phi(x)\delta(x - x_i) \tag{22}$$

subject to the homogeneous boundary conditions

$$-k_1\phi(0) + \frac{\mathrm{d}\phi(0)}{\mathrm{d}x} = 0, \qquad k_2\phi(1) + \frac{\mathrm{d}\phi(1)}{\mathrm{d}x} = 0$$

There exists a countably infinite number of eigenfunctions $\phi_r(x)$ $(r = 1, 2, \ldots)$ and associated eigenvalues λ_r that solve Eq. (18). In the absence of feedback control [letting $g_i = h_i = 0\,(i = 1, 2, \ldots, n)$ in Eq. (22)] the eigensolutions are

$$\begin{aligned}\phi_r^0(x) &= N_r(k_1 \sin\beta_r x + \beta_r \cos\beta_r x)\\ \lambda_r^0 &= i\beta_r\sqrt{AE/m} \qquad (r = 1, 2, \ldots)\end{aligned} \tag{23}$$

in which β_r satisfy the characteristic equation $0 = (k_1 k_2 - \beta_r^2)\tan\beta_r + (k_1 + k_2)\beta_r$, the normalization constants are

$$N_r = \left[\frac{1}{2}\left(k_1^2 + b_r^2\right) + \left(\frac{-k_1^2 + b_r^2}{4b_r}\right)\sin 2b_r + \frac{kA}{2}(1 - \cos 2b_r)\right]^{-\frac{1}{2}}$$

and the superscript 0 designates quantities associated with the uncontrolled system. The eigenfunctions of the uncontrolled system are also referred to as natural modes of vibration. The eigenfunctions of the controlled system are also called controlled modes of vibration. The locations of the forces x_i $(i = 1, 2, \ldots, n)$ and the control gains g_i and h_i $(i = 1, 2, \ldots, n)$ are determined on the basis of the following node control conjecture.

Node control conjecture: A uniform bar with homogeneous boundary conditions in which the lowest n natural modes of vibration participate significantly in the system response, when subject to n direct state feedback forces placed at the zeros of the $(n+1)$th natural mode, can be controlled in a manner that satisfies the following three properties.

1) Mode invariance: the n controlled modes of vibration are identical to the natural modes of vibration.

2) Frequency invariance: the frequencies of oscillation of the n controlled modes of vibration are identical to the natural frequencies of oscillation.

3) Uniform damping: the damping rates of the n controlled modes of vibration are identical to each other.

The desirability associated with these three properties was described in detail in Ref. 4. In short, the first two properties minimize the magnitude of the direct feedback control forces. Control forces increase in magnitude when tasked to effectively change the bar's natural modes of vibration and to change the bar's natural frequencies of oscillation. We can see that the third property is desirable when we consider the alternatives. The allowance of one decay rate to be lower than the others yields a response that in time is dominated by that mode. Furthermore, the magnitude of a control force increases with the decay rate. It follows that the control forces will be unnecessarily large when one decay rate is either smaller or larger than the rest. The level of uniform damping is then selected on the basis of how much overall effort associated with the control forces the designer is willing to expend.

It is now shown how the node control conjecture follows from the orthogonal function conjecture. First express the n lowest controlled modes in terms of the lowest n natural modes as

$$\phi_r(x) = \sum_{s=1}^{n}\phi_s^0(x)c_{rs} \qquad (r = 1, 2, \ldots, n) \tag{24}$$

in which c_{rs} $(r, s = 1, 2, \ldots, n)$ are called coupling coefficients. Equation (24) is tantamount to assuming that n modes participate in the system response and that the participation of the remaining modes is negligible. Substituting Eq. (24) into Eq. (22), premultiplying by

$$\frac{1}{m}\int_0^1 \phi_r^0(x)(\,)\,\mathrm{d}x$$

and applying the orthonormality conditions (1) yields the eigenvalue problem

$$\begin{aligned}0 = \sum_{s=1}^{n}\Bigg\{&\lambda_r^2\delta_{st} + \lambda_r\frac{1}{m}\left[\sum_{i=1}^{n}h_i\phi_s^0(x_i)\phi_t^0(x_i)\right] + \lambda_s^{02}\delta_{st}\\ &+ \frac{1}{m}\left[\sum_{i=1}^{n}g_i\phi_s^0(x_i)\phi_t^0(x_i)\right]\Bigg\}c_{rs} \qquad (r, t = 1, 2, \ldots, n)\end{aligned} \tag{25}$$

It follows from the orthogonal function conjecture that the parenthetic summations in Eq. (25) can be reduced to the form

$$\sum_{i=1}^{n}h_i\phi_s^0(x_i)\phi_t^0(x_i) = h\delta_{st}, \qquad \sum_{i=1}^{n}g_i\phi_s^0(x_i)\phi_t^0(x_i) = g\delta_{st} \qquad (s, t = 1, 2, \ldots, n) \tag{26}$$

Substituting Eq. (26) into Eq. (25) yields

$$0 = \left[\lambda_r^2 + \lambda_r(h/m) + \lambda_t^{02} + (g/m)\right]c_{rt} = 0 \qquad (r, t = 1, 2, \ldots, n) \tag{27}$$

Solving Eq. (27) yields

$$c_{rt} = \delta_{rt} \qquad (r, t = 1, 2, \ldots, n) \qquad \text{and} \qquad \lambda_r = -\alpha \pm i\omega_r^0 \tag{28}$$

in which $\alpha = (h/2m)$ is the uniform decay rate and $\omega_r^0 = \sqrt{(-\lambda_r^0)}$ is the rth natural frequency of oscillation. Indeed, Eq. (28) is a statement of the three properties predicted by the node control conjecture.

Summary

This Note introduced an unproven conjecture about orthogonal functions. The conjecture leads to a paradox that is currently unresolved except in case of the orthogonal functions $\phi_r(x) = \sqrt{2}\sin r\pi x$ $(r = 1, 2, \ldots)$. The application of the conjecture to the control of distributed systems was also presented in the form of a node control conjecture.

References

[1] Weaver, L., Jr., and Silverberg, L., "Node Control of Uniform Beams Subject to Various Boundary Conditions," *Journal of Applied Mechanics*, Vol. 59, Dec. 1992, pp. 983–990.

[2] Rosetti, D. J., and Sun, J. Q., "Uniform Modal Damping of Rings by an Extended Node Control Theorem," *Journal of Guidance, Control, and Dynamics*, Vol. 18, No. 2, 1995, pp. 373–375.

[3]Bokar, J., Silverberg, L., and Özisik, M. N., "An Engineering Foundation for Controlling Heat Transfer in One-Dimensional Transient Heat Conduction Problems," *International Communications in Heat and Mass Transfer*, Vol. 22, No. 6, 1995, pp. 849–858.

[4]Silverberg, L., "Uniform Damping Control of Spacecraft," *Journal of Guidance, Control, and Dynamics*, Vol. 9, No. 2, 1986, pp. 221–227.

Disturbance Rejection Approach to Actuator and Sensor Placement

K. B. Lim*
NASA Langley Research Center,
Hampton, Virginia 23681-0001

I. Introduction

FOR various reasons as discussed elsewhere,[1] the selection of actuator and sensor positions is still ad hoc. This is especially true for flexible structures, for which many candidate configurations can exist. This study is an attempt to make the selection process more methodical.

One approach to actuator and sensor placement is to optimize a closed-loop performance metric directly by selecting the actuators, sensors, and controller gains simultaneously. This direct approach makes sense if the desired closed-loop performance is well defined. Because the individual actuator and sensor contributions to the closed-loop performance metric are complex, the solution strategy usually employs nonlinear programming with many design and numerical iterations. A second approach is to select actuators and/or sensors on the basis of open-loop properties so that closed-loop performance is indirectly optimized. Because the individual sensor and actuator contributions to the open-loop metric are simple, nonlinear optimization usually is not needed. This approach will suggest efficient actuator and sensor configurations for any type of control law. The suggested method falls into the latter class of approaches.

The use of a Hankel singular value (HSV) formula as an actuator placement metric[2] is extended to flexible structures in discrete time.[3] A main novelty introduced is that the ambiguity in the weighting of the principal modes is addressed by incorporating the general disturbance rejection goal into the actuator and sensor placement formulation. Optimal actuator and sensor placement is considered for the purpose of designing control laws for the general disturbance rejection problem. This apparent restriction to the disturbance rejection problem is not too restrictive because it is well known from modern multivariable control theory that stability and even robustness requirements can be transformed to this form with appropriate weighting. Simulation results demonstrate that the improvement in closed-loop performance is independent of the type of controller used because open-loop properties have been improved.

II. Actuators and Sensors for Disturbance Rejection

Figure 1 shows a schematic of the disturbance rejection problem where the inputs to the plant consist of two vectors and, similarly, the outputs consist of two vectors. As a necessary starting point in a disturbance rejection problem, the disturbance source (or inputs) and the output response defining the performance to be optimized usually are defined by the requirements of the control problem.

The disturbance rejection viewpoint taken in this study is similar to the mode selection viewpoint proposed earlier in the context of model reduction for flexible structures.[4] The preceding formulation is also consistent with the general multivariable control design,[5] in which the plant $P = [P_{11}, P_{12}; P_{21}, P_{22}]$ is assumed to be given and the problem is to design a stabilizing and realizable controller, K, to minimize a suitable norm of the closed-loop transfer function matrix, $F_l(P, K)$. The basic difficulty in the actuator and sensor placement problem is that only P_{11} is given.

HSVs are used to construct a metric that quantifies the degree of controllability and observability for a given set of sensor and actuator configurations. Although the use of HSV to analyze the degree of controllability and observability of a linear system is well established, especially in model reduction applications,[4,6,7] the approximate decomposition of the HSV with multiple sensors and actuators in terms of the HSV of all combinations of sensor-actuator pairs is new. This result significantly simplifies the design problem of selecting the most effective set of sensors and actuators for flexible structures. The main novelty of the placement strategy is that the HSVs from the disturbance to the performance outputs are used to weigh the HSVs between candidate actuator and sensor sets. This is possible because, in both cases, individual HSVs directly correspond to individual structural modes, which is unique to flexible structures.

III. Decomposition of HSV

Given the quadruple (A_z, B_z, C_z, D_z) of a discrete linear time-invariant state-space matrix of a flexible structure, assumed to be lightly damped with distinct eigenvalues, let $(\tilde{A}, \tilde{B}, \tilde{C}, \tilde{D})$ denote the 2×2 block diagonal form whose ith block is

$$\tilde{A}_i = \begin{bmatrix} \mathrm{Re}(z_i) & -\mathrm{Im}(z_i) \\ \mathrm{Im}(z_i) & \mathrm{Re}(z_i) \end{bmatrix} \tag{1}$$

where (z_i, v_i) denote the ith eigenvalue and eigenvector pair of A_z, and let T denote the sampling period. The steady-state discrete-time controllability gramian $W_{c\infty}$ and the observability gramian $W_{o\infty}$ satisfy the Sylvester equations. The triple $(\tilde{A}, \tilde{B}, \tilde{C})$ is internally balanced if its gramians are equal and diagonal,[7] i.e., $W_{c\infty} = W_{o\infty} = \Gamma^2$. The nonnegative real diagonal elements of Γ^2 are called the HSVs of the system.

Because of the diagonal dominance property of the discrete controllability and observability gramian for flexible structures, the square of the ith HSV[3] is given by

$$\gamma_i^4 \cong \frac{\mathrm{tr}[\tilde{B}\tilde{B}^T]_{ii}\ \mathrm{tr}[\tilde{C}^T\tilde{C}]_{ii}}{(4\delta_i T)^2} \tag{2}$$

where $\delta_i = -(1/T)\mathrm{Re}(\ell n z_i)$ and the subscript ii denotes the ith 2×2 block of matrices formed from the inputs and outputs. It is shown[3] that the approximate formula is quite accurate up to frequencies near 90% of the Nyquist frequency.

For p actuators and q sensors, the input and output matrices consist of p columns and q rows, respectively:

$$B_z = \left[B_{z_1}, \ldots, B_{z_p}\right]; \qquad C_z^T = \left[C_{z_1}^T, \ldots, C_{z_q}^T\right] \tag{3}$$

Partition the state transformation matrix as follows:

$$V = [r_1, \ldots, r_n]; \qquad V^{-T} = \left[l_1^T, \ldots, l_n^T\right] \tag{4}$$

where $r_i = [\mathrm{Re}(v_i), -\mathrm{Im}(v_i)]$ and l_i^T are $2n \times 2$ matrices made up of components of ith right and left eigenvectors. The approximate

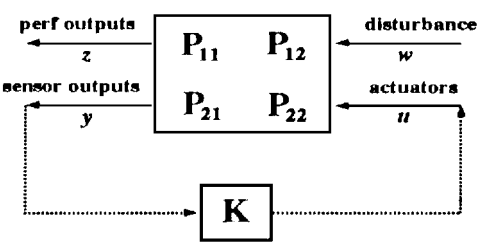

Fig. 1 General disturbance rejection problem.

Received March 4, 1996; revision received May 3, 1996; accepted for publication June 24, 1996.

*Research Engineer, Guidance and Control Branch, Flight Dynamics and Controls Division, MS 161.